Wind System Based on a Doubly Fed Induction Generator: Contribution to the Study of Electrical Energy Quality and Continuity of Service in the Voltage Dips Event

Ibtissam Kharchouf*‡, Ahmed Essadki*, Tamou Nasser**

*Higher School of Technical Education ENSET- Mohammed V University - Rabat- Morocco

** National School of Computer Science and Systems Analysis ENSIAS- Mohammed V University - Rabat- Morocco

(ibtissam.kharchouf@um5s.net.ma, ahmed.essadki1@gmail.com, tnasser@ensias.ma)

‡ Corresponding Author; Ibtissam KHARCHOUF, Morocco, Tel: +212 630 647 763.

Received: 10.04.2017 Accepted:22.05.2017

Abstract- Industrial machines are very sensitive to electrical defects especially the Doubly Fed Induction Generators. This high sensitivity reveals many difficulties in terms of compliance with the specifications imposed by the electrical grid operators. This article gives a proposed strategy to control the whole wind conversion chain which allows to obtain high production performances in perturbed conditions (the voltage dips). To do this, a comparison between two control strategies, one conventional and the other modified, is presented to conclude about which one guarantees a good electrical energy quality and continuity of service in the voltage dips event. The results of this work are provided by simulations in the MATLAB / SIMULINK environment.

Keywords Conventional Control Strategy, Doubly Fed Induction Generator (DFIG), Modified Control Strategy, Voltage Dips, Wind Turbine.

1. Introduction

Voltage dip may cause very harmful problems even if it is relatively small. This defect for the industrialist and entrepreneurs means, production stoppages, overtime for restarting processes which causes performances degradation. And to have a close idea about the disturbance costs; the dissatisfaction of customers, the risks to the safety and security of staff and of the production tools, the loss of data, etc, must also be considered [15].

To avoid all the consequences mentioned before, and any instability in the production of electrical energy, a continuation of wind turbine production even in disturbed conditions, must be assured.

The objective of this research article is to propose a control strategy of the generator that can improves the performances of the wind systems in the case of a disturbed electrical grid. The emphasis is on the comparison of two stator flux control strategies (conventional and modified) of the DFIG (Doubly Fed Induction Generator) [2], [3]. On the one hand, the conventional approach allows to obtain the mode of operation sought by positioning in an optimal way the currents vectors and the resulting flows vectors. On the other hand, the modified approach considers the dynamics of the stator flux [3]. The fault current in the rotor windings and the overvoltage in the DC bus are limited due to the proposed control strategy.

The wind generator used is a three-axis horizontal wind turbine using a Doubly Fed Induction Generator (DFIG).

Nomenclatures

PWM	Pulse Width Modulation.
C_r	Resistive torque (N.m).
C_{aer}	Aerodynamic torque (N.m).
C_{mec}	Mechanical torque (N.m).
Ω_t	Turbine speed (Rad/s).

Ω_{mec}	Mechanical Speed (Rad/s).
Ω_{ref}	Reference speed (Rad/s).
V_v	Wind speed (m/s).
s	Stator axes index.
r	Rotor axes index.
i_{rm}	The current supplied by the generator (A).
i_c	The current through the capacitor (A).
I_{gm}	The current modulated by the PWM converter.
i_{sd}	Stator currents on the d axis (A).
i_{sq}	Stator currents on the q axis (A).
i_{rd}	Rotor currents on the d axis (A)
i_{td}	Direct component of the filter current (A).
i_{tq}	Quadrature component of the filter current (A).

2. Vector Control of the DFIG

To obtain the desired mode of operation, a vector control is recommended by optimally positioning the current vectors and the resulting flux vectors, [2], [3], [8].

The architecture of the control device is given in Fig. 1, it can be divided in two parts:

- Controlling the active and reactive powers produced by the machine through the rotor side converter (RSC).
- Monitoring the DC bus voltage and the power factor rated network via the grid side converter (GSC)

2.1. The DFIG model

The particularity of a DFIG is that it has two currents to control directly ird and irq, and two currents indirectly controlled isd and isq.

- Let's recall the differential equations system of the machine [4]:

$$V_{sd} = R_s.I_{sd} - \omega_s.\psi_{sq} + \frac{d\psi_{sd}}{dt} \tag{1}$$

$$V_{sq} = R_s.I_{sq} + \omega_s.\psi_{sd} + \frac{d\psi_{sq}}{dt} \tag{2}$$

$$V_{rd} = R_r.I_{rd} - \omega_r.\psi_{rq} + \frac{d\psi_{rd}}{dt} \tag{3}$$

$$V_{rq} = R_r.I_{rq} + \omega_r.\psi_{rd} + \frac{d\psi_{rq}}{dt} \tag{4}$$

- Flux's relations:

$$\psi_{sd} = L_s.I_{sd} + M.I_{rd} \tag{5}$$

$$\psi_{sq} = L_s.I_{sq} + M.I_{rq} \tag{6}$$

$$\psi_{rd} = L_r.I_{rd} + M.I_{sd} \tag{7}$$

$$\psi_{rq} = L_r.I_{rq} + M.I_{sq} \tag{8}$$

A vector control of this machine was designed by orienting the Park's frame, so that the stator flux along the d axis is constantly zero (ψ_{sq} =0), Which simplifies the DFIG obtained model and the resulting control device [5].

Equations (1 and 2) become:

$$\frac{d\psi_{sd}}{dt} = V_{sd} - R_s.I_{sd} \tag{9}$$

$$V_{sq} = R_s.I_{sq} + \omega_s.\psi_{sd} \tag{10}$$

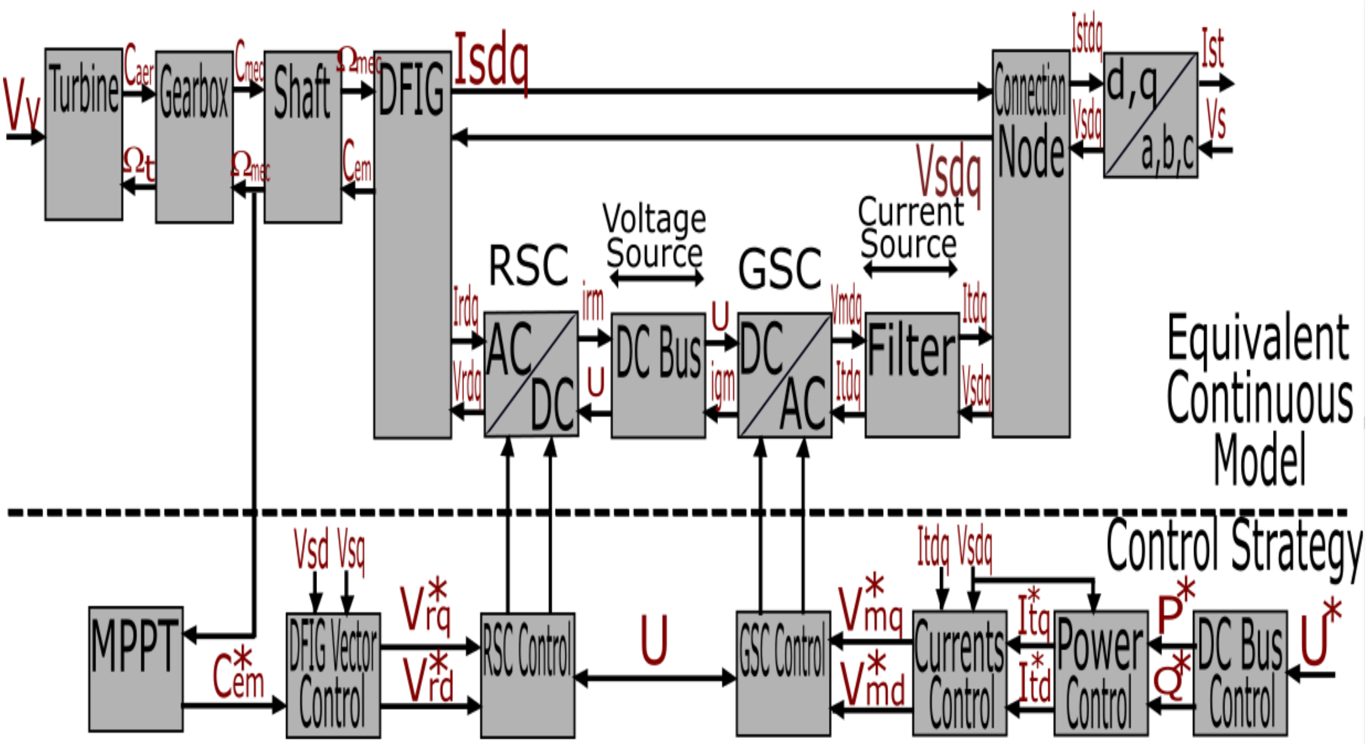

Fig. 1. The control device of a variable speed wind turbine based on the DFIG

$$\frac{d\psi_{rd}}{dt} = V_{rd} - R_r.I_{rd} + \omega_r.\psi_{rq} \quad (11)$$

$$\frac{d\psi_{rq}}{dt} = V_{rq} - R_r.I_{rq} - \omega_r.\psi_{rd} \quad (12)$$

From the equations of the direct and quadrature stator flux components, we obtain the following expressions of the stator currents [5]:

$$I_{sq} = -\frac{M}{L_s}.I_{rq} \quad (13)$$

$$I_{sd} = \frac{\psi_{sd} - M.I_{rd}}{L_s} \quad (14)$$

These stator currents are replaced in the equations of the direct and quadrature rotor fluxes components (7 and 8):

$$\psi_{rd} = L_r.\sigma.i_{rd} + \frac{M}{Ls}.\psi_{sd} \quad (15)$$

$$\psi_{rq} = L_r.\sigma.i_{rq} \quad (16)$$

σ is the dispersion coefficient between the dq windings:

$$\sigma = 1 - \frac{M^2}{L_s.L_r} \quad (17)$$

By replacing the expressions of the direct and quadrature stator currents components (13 and 14) in equations (9 and 10) and the expressions of the direct and quadrature rotor fluxes components (15 and 16) in equations (11 and 12), [2], [7] we obtain:

$$V_{sd} = \frac{R_s}{L_s}.\psi_{sd} - \frac{R_s}{L_s}.M.I_{rd} + \frac{d\psi_{sd}}{dt} \quad (18)$$

$$V_{sq} = -\frac{R_s}{L_s}.M.I_{rq} + \omega_s.\psi_{sd} \quad (19)$$

$$V_{rd} = R_r.I_{rd} + L_r.\sigma.\frac{dI_{rd}}{dt} + \frac{M}{L_s}\frac{d\psi_{sd}}{dt} - L_r.\omega_r.\sigma.I_{rq} \quad (20)$$

$$V_{rq} = R_r.I_{rq} + L_r.\sigma.\frac{dI_{rq}}{dt} + L_r.\omega_r.\sigma.I_{rd} + \omega_r.\frac{M}{L_s}.\psi_{sd} \quad (21)$$

The rotor equations (20 and 21) permit to determine the rotor currents:

$$\frac{dI_{rd}}{dt} = \frac{1}{L_r.\sigma}.(V_{rd} - R_r.I_{rd} - e_q) \quad (22)$$

$$\frac{dI_{rq}}{dt} = \frac{1}{L_r.\sigma}.(V_{rq} - R_r.I_{rq} - e_d - e_\psi) \quad (23)$$

Where the EMFs are defined as:

$$e_q = -L_r.\omega_r.\sigma.I_{rq} + \frac{M}{L_s}.\frac{d\psi_{sd}}{dt} \quad (24)$$

$$e_\psi = \omega_r.\frac{M}{L_s}.\psi_{sd} \quad (25)$$

$$e_d = L_r.\omega_r.\sigma.I_{rd} \quad (26)$$

The torque's expression:

$$\mathrm{T}_{em} = p.(\psi_{sd}.I_{sq} - \psi_{sq}.I_{sd}) \quad (27)$$

By orienting the stator flux (ψ_{sq} = 0), we obtain a simplified torque expression:

$$\mathrm{T}_{em} = p.\psi_{sd}.I_{sq} \quad (28)$$

By using the equation (13), The torque then becomes proportional to the quadrature axis current component [2], [3], [6], thus the torque control is carried out from the current I_{rq} regulation:

$$\mathrm{T}_{em} = -p.\frac{M}{L_s}\psi_{sd}.I_{rq} \quad (29)$$

The direct stator voltage component is close to zero. Thus, the reactive power can be described by:

$$Q_s = V_{sq}.I_{sd} = \frac{V_s.\psi_s}{L_s} - \frac{V_s.M}{L_s}I_{rd} \quad (30)$$

We remark that the reactive power can be controlled by regulating the direct rotor current component I_{rd}.

Remarks:

- By chosen the dq axes as a reference (ψ_{sd} is maintained constant), the electromagnetic torque produced by the DFIG and consequently the stator power become proportional to the quadrature component of the rotor current I_{rq}.
- The stator reactive power is not proportional to the direct rotor current due to a constant imposed by the grid $\frac{V_s.\psi_s}{L_s}$.
- The two stator powers can be controlled independently.

2.2. Control strategy of the DFIG rotor currents

The simplified representation of the current regulation in a block diagram form is given in Fig. 2.

At the end of these settings, we obtain $I_{rq} = I_{rq-ref}$ and $I_{rd} = I_{rd-ref}$ with a chosen response time (the speed loop response time chosen to be superior to the currents response time) [2], [3].

2.2.1. Flux estimation

The direct stator flux component is written by:

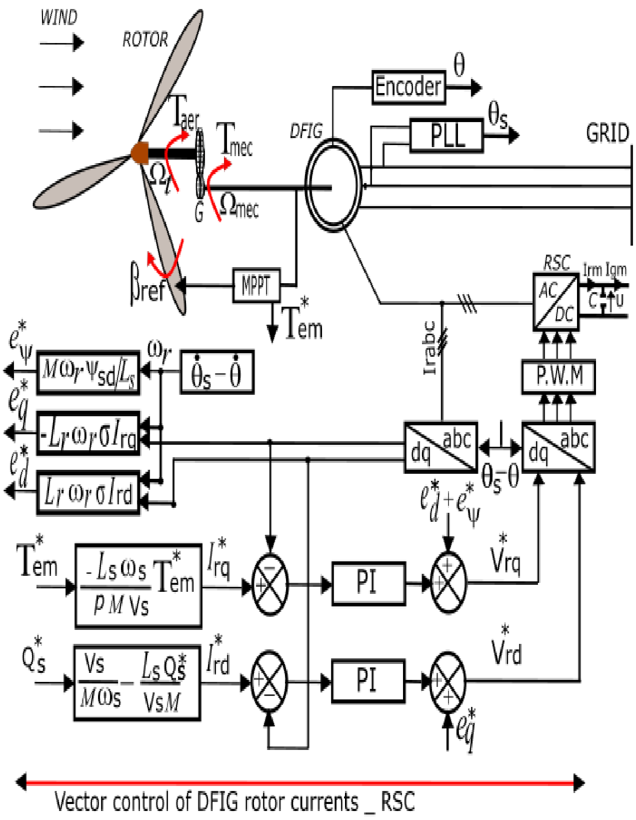

Fig. 2. The RSC control strategy

$$\psi_{sd} = L_s.I_{sd} + M.I_{rd} \tag{31}$$

This flux can be estimated from the currents measurement I_{sd} and I_{rd} [2].

2.2.2. Generation of the rotor currents references

The rotor current reference is obtained by a constant multiplied by the electromagnetic torque T_{em-ref}, issuing from the MPPT control block, by:

$$I_{rq-ref} = -\frac{L_s.\omega_s}{p.M.V_s} T_{em-ref} \tag{32}$$

The flux amplitude is controllable by I_{rd} [2]. In the case of this article we generate I_{rd-ref} to operate at zero reactive power.

The direct rotor current reference is obtained from (30), and it's generated to operate at $Q_{s-ref} = 0$.

$$I_{rd-ref} = \frac{V_s}{M.\omega_s} - \frac{L_S}{V_s.M} Q_{s-ref} \tag{33}$$

In this study, a PI controller was used to control the DFIG. Due to its implementation simplicity while offering acceptable performances.

2.3. Control strategy of the grid connection

The purpose from controlling the GSC is to maintain a constant DC bus voltage whatever the amplitude and the direction of power, and to guarantee a required power factor.

The GSC controls the currents flown by the filter and the vector control allows an independent and decoupled control of the active and reactive powers circulating between the grid and the GSC. The currents are controlled by two regulators which generate the applied voltages references (V_{md-ref} and V_{mq-ref}). The quadrature axis current is used to regulate the DC bus voltage and the direct axis current to regulate the reactive power [2], [3], [9].

2.3.1. Control strategy of the currents sent to the grid

The filter model can be simplified by the following equations:

$$V_{md} = R_t I_{td} + L_t \frac{dI_{td}}{dt} - e_{tq} \tag{34}$$

$$V_{mq} = R_t I_{tq} + L_t \frac{dI_{tq}}{dt} + e_{td} + V_s \tag{35}$$

Where,

$$e_{tq} = L_t.\omega_s.I_{tq} \tag{36}$$

$$e_{td} = L_t.\omega_s.I_{td} \tag{37}$$

R_t and L_t are the filter resistance and inductance respectively.

We can set up a control of the circulating currents in the RL filter, assuring a decoupled control for each axis. The RL filter currents of the dq axes are the controllers reference's values [2], [3].

I_{tq-ref} and I_{td-ref} are respectively derived from the control block of the DC bus voltage and the reactive power control [2], [3].

The control device contains three specific actions:

- A voltage compensation:

$$e_{q-ref} = L_t.\omega_s.I_{tq} \tag{38}$$

$$e_{d-ref} = L_t.\omega_s.I_{td} \tag{39}$$

- A decoupling action of the currents:

$$V_{md-ref} = V_{bd-ref} - e_{tq-ref} \tag{40}$$

$$V_{mq-ref} = V_{bq-ref} + e_{td-ref} + v_{sq} \tag{41}$$

- Closed loop control of currents:

$$V_{bd-ref} = C_i.(i_{td-ref} - i_{td}) \tag{42}$$

$$V_{bq-ref} = C_i.(i_{tq-ref} - i_{tq}) \tag{43}$$

2.3.2. Power control

By neglecting R_t and considering $(V_{sd} = 0)$,The powers exchanged through the filter to the grid become:

$$P_t = V_{sq}.I_{tq} \tag{44}$$

$$Q_t = V_{sq}.I_{td} \tag{45}$$

We obtain I_{tq-ref} and I_{td-ref} from the previous relations:

$$I_{tq-ref} = \frac{P_{t-ref}}{V_{sq}} \tag{46}$$

$$I_{td-ref} = \frac{Q_{t-ref}}{V_{sq}} \tag{47}$$

I_{td-ref} is used to control the reactive power at the GSC connection point with the electrical grid. I_{tq-ref}, for its part, is used to maintain the DC bus voltage constant. With this principle, a null reference reactive power can then be imposed $Q_{t-ref} = 0VAR$.

2.3.3. DC bus control

From $I_c = I_{rm} - I_{gm}$, we can express the powers involved in the DC bus:

$$P_r = U.I_{rm} \tag{48}$$

$$P_c = U.I_c \tag{49}$$

$$P_g = U.I_{gm} \tag{50}$$

These powers are linked by the relation:

$$P_g = P_r + P_c \tag{51}$$

If we neglect all Joules losses (losses in the capacitor, the converter and the RL filter), The power outcoming from the grid P_t corresponds to the power outcoming from the DC bus added to the power appearing in the rotor circuit P_r, in hypersynchronous mode:

$$P_t = U.i_{dc} + P_r \tag{52}$$

The capacitor current is used to regulate the DC bus voltage by a PI controller.

The block diagram of the corresponding control is shown in Fig. 3. The voltages are then sent to a PWM modulator.

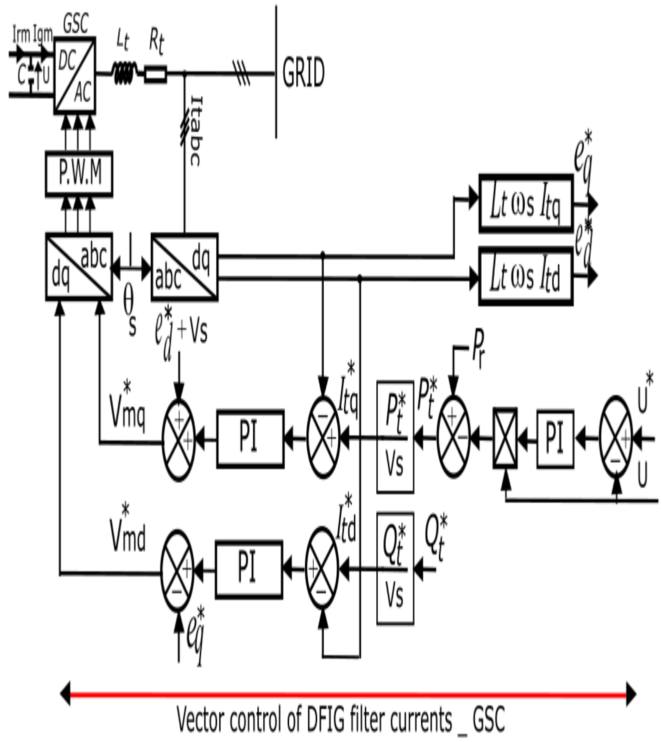

Fig. 3. The GSC control strategy

3. Modified Vector Control Strategy of the DFIG

In the conventional vector control the flux is taken as a constant to simplify the dimensioning of the current controllers while controlling the DFIG. However, during a voltage dip, the stator flux will decrease because the stator is directly connected to the grid. Moreover, the calculation of the Park's orientation frame may be distorted during the voltage dip. As a solution, the stator flux dynamics must not be neglected during the dimensioning of the current controllers [3].

The stator flux components are expressed as:

$$\Psi_{sd} = L_s.I_{sd} + M.I_{rd} \tag{53}$$

$$\Psi_{sq} = L_s.I_{sq} + M.I_{rq} \tag{54}$$

During a voltage dip, the quadrature stator flux component is not null. This implies that the stator currents are obtained by:

$$I_{sq} = \frac{\Psi_{sq} - M.I_{rq}}{L_s} \tag{55}$$

$$I_{sd} = \frac{\Psi_{sd} - M.I_{rd}}{L_s} \tag{56}$$

By replacing these equations in the expressions of the rotor fluxes, we obtain:

$$\Psi_{rd} = L_r.\sigma.i_{rd} + \frac{M}{Ls}.\Psi_{sd} \tag{57}$$

$$\psi_{rq} = L_r.\sigma.i_{rq} + \frac{M}{Ls}.\psi_{sq} \quad (58)$$

By replacing the currents equations (55 and 56) in the expressions of the stator voltages (1 and 2) we obtain:

$$V_{sd} = \frac{R_s}{L_s}.\psi_{sd} - \frac{R_s}{L_s}.M.I_{rd} + \frac{d\psi_{sd}}{dt} \quad (59)$$

$$V_{sq} = \frac{R_s}{L_s}.\psi_{sq} - \frac{R_s}{L_s}.M.I_{rq} + \frac{d\psi_{sq}}{dt} \quad (60)$$

And by replacing the expressions of the rotor flux (57 and 58) in the expressions of the rotor voltages (3 and 4), we obtain:

$$V_{rd} = R_r.I_{rd} + L_r.\sigma.\frac{dI_{rd}}{dt} + e_q + e_{\psi d} \quad (61)$$

$$V_{rq} = R_r.I_{rq} + L_r.\sigma.\frac{dI_{rq}}{dt} + e_d + e_{\psi q} \quad (62)$$

with:

$$e_q = -L_r.\omega_r.\sigma.I_{rq} \quad (63)$$

$$e_d = L_r.\omega_r.\sigma.I_{rd} \quad (65)$$

$$e_{\psi d} = \frac{M}{L_s}(-\omega_r\psi_{sq} + \frac{d\psi_{sd}}{dt}) \quad (66)$$

$$e_{\psi q} = \frac{M}{L_s}(\omega_r\psi_{sd} + \frac{d\psi_{sq}}{dt}) \quad (67)$$

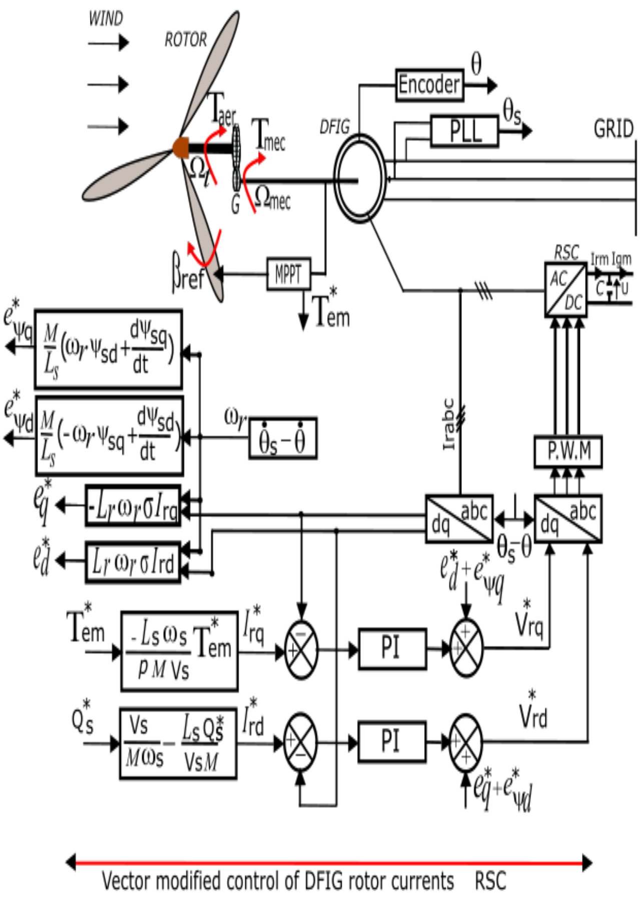

Fig. 4. The DFIG modified vector control strategy

From these equations, we can dimension a PI controller for the rotor currents. It should be noted that for a correct control the stator flux and its dynamics $(\frac{d\psi_{sd}}{dt}, \frac{d\psi_{sq}}{dt})$ must be compensated during the voltage dip.

4. Simulation Results

To study the influence of the voltage dips on the proposed strategy, a three-phase voltage dip of 20% and for duration of 100 ms is applied to the DFIG. The system model and its control were simulated using Matlab/Simulink considering a 1.5 MW DFIG and a constant wind speed of 13 m/s. The system parameters are summarized in Table 1, Table 2 and Table 3.

Table 1. DFIG and wind turbine Parameters

DFIG Parameters	
Nominal Power	1.5 MW
Stator Resistance (R_s)	Rs=0.012 Ω
Rotor Resistance (R_r)	Rr=0.021 Ω
Stator Inductance (L_s)	Ls=0.0137 H
Magnetization Inductance (M)	M=0.0135 H
Rotor Inductance (L_r)	Lr=0.0136 H
Number of pole pairs (P)	P=2
Friction Coefficient (f)	f= 0.0024 N.m.s-1
Power Supply Frequency (F)	F=50 Hz
Wind turbine parameters	
Blade number	3
Blade radius (R)	R=35.25 m
Gear-box gain (G)	G=90
Inertia (J)	J=1000 Kg.m2

Table 2. Parameters of the different wind system commands

Rotor currents control	Time constant in closed loop $\tau = 1ms$ $K_i = \frac{R_r}{\tau} = 21$ $K_p = \frac{\sigma.L_r}{\tau} = 0.297$
Filter currents control	Time constant in closed loop $\tau = 1ms$ $K_i = \frac{R_t}{L_t} = 2.4$ $K_p = \frac{L_t}{\tau} = 5$
DC bus voltage control	Damping factor: $\xi = 0.707$ Cut-off frequency: $\omega_n = 27rad/s$ $K_p = 2\xi C\omega_n = 0.167$ $K_i = C\omega_n^2 = 3.2076$

Table 3. Parameters of the RL filter and the DC bus

Parameters of the RL filter	
Resistance R_t	0.012 Ω
Inductance L_t	0.005 H
Parameters of DC bus	
Capacitor C	C=0.0044 F
Voltage U_{dc}	U_{dc}=1200 V

When the fault occurs at t=0.6s, the generator voltage drops for a duration of t=100ms and it gets back to its reference at t=0.8s as shown in figure. 5. The voltage dip fault leads to decrease the stator flux and it causes a non-stability which means the stator flux in the quadrature axis cannot be maintained at zero. That is why, the stator flux and its dynamics cannot be neglected.

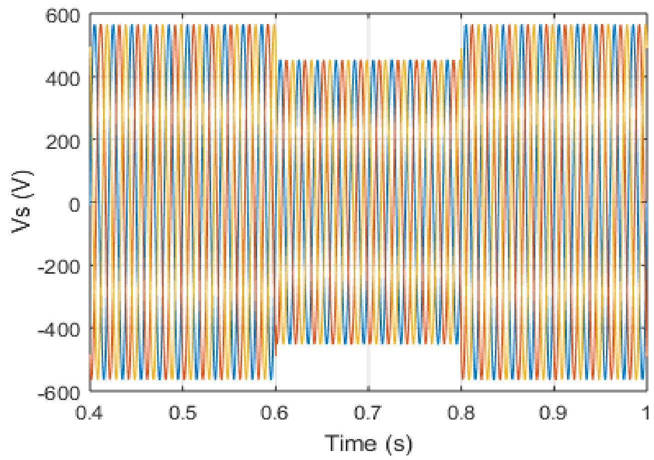

Fig. 5. The grid voltages during a three-phase voltage dip

The stator currents have different amplitudes during the voltage dip. The fault current amplitude obtained between t=0.6s and t=0.8s with the classical (conventional) approach Fig. 6(b) is higher than the amplitude obtained with the modified approach during the fault Fig. 6(a). The generated amplitude depends on the saturation curve of the generator.

In practice, the currents generated during a voltage dip are reduced after their detection by means of a short-circuit system located at the rotor.

The fact of having an imbalance of the three-phase stator currents strongly causes an imbalance in the total current sent by the DFIG.

The amplitude of the three-phase rotor currents has been modified during the voltage dip. At t=0.6s the conventional control can't keep the rotor currents at their steady state value as shown in Fig .7(b). The rotor currents amplitude during the fault is lower with the modified control strategy Fig. 7(a).

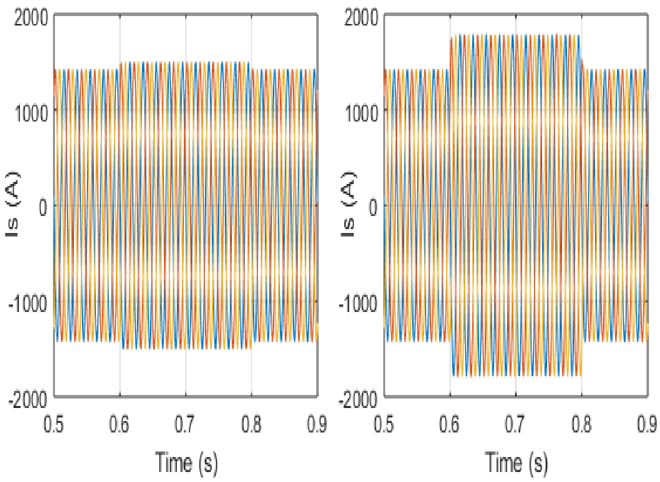

(a) Stator currents with the modified approach

(b) Stator currents with the conventional approach

Fig. 6. The DFIG stator currents

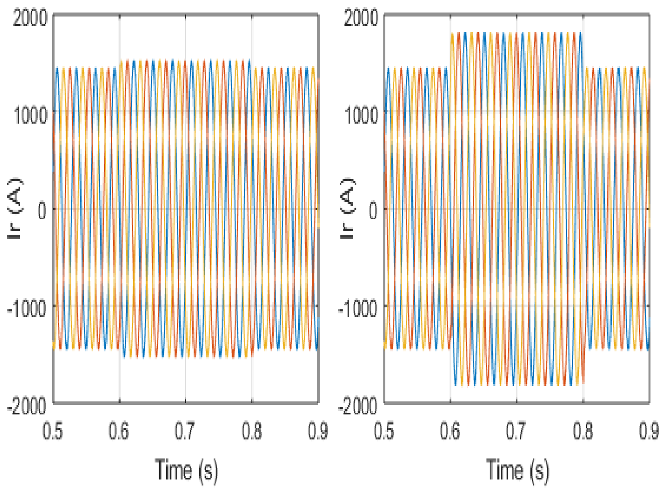

(a) Rotor currents with the modified approach

(b) Rotor currents with the conventional approach

Fig. 7. The DFIG rotor currents

As shown in Fig. 8 the DC bus voltage is oscillating with a smaller amplitude with the modified control, this is due to the stator flux dynamics consideration. These oscillations affect the total active powers sent to the grid.

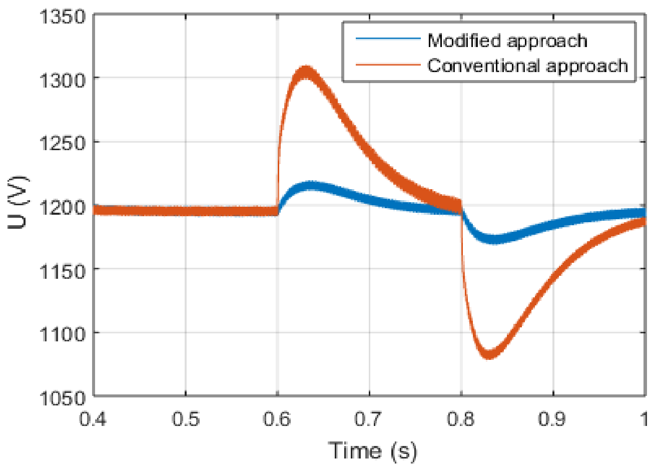

Fig. 8. DC bus voltage during a voltage dip

With the same wind profile, the active powers exchanged with the grid are different when the stator flux is changed during the fault (the same remark about the mechanical speed). We obtain a higher power with the modified approach than with the conventional approach Fig. 9. It can also be noted that the decrease of this power during the voltage dip is greater using the conventional approach.

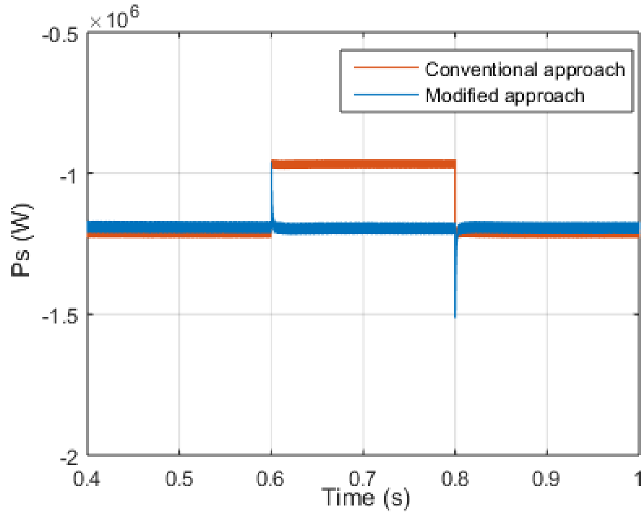

Fig. 9. The stator active powers

The total reactive power is oscillating with a bigger amplitude using the conventional method Fig. 10. The reactive power using the modified control is close to zero to maintain a unit power factor Fig. 10.

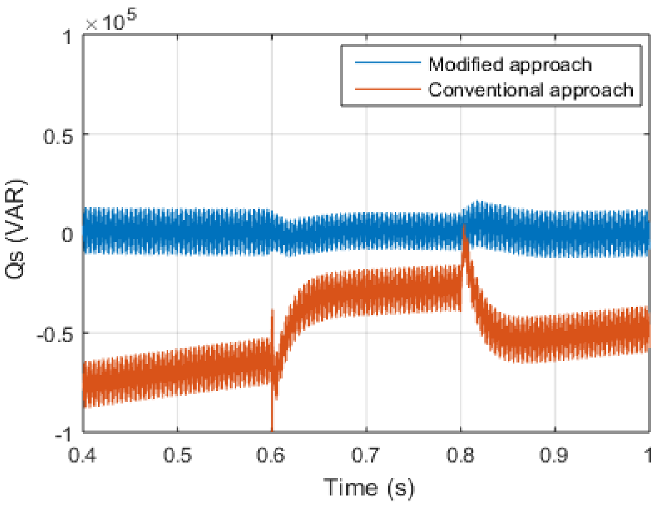

Fig. 10. The stator reactive powers

5. Conclusion

The work carried out in this article had as an objective the elaboration of a complete control strategy of the wind turbines using a DFIG in the normal (stable) electrical grid and abnormal (voltage dip) cases. To achieve this objective, for the normal case a conventional vector control has been presented to show the machine remarkable performances. A decoupled control of the active and reactive powers (also of the power factor) has been obtained and improved the quality of the energy supplied to the grid.

Then a modified vector control strategy of the device was proposed, which considers the stator flux dynamics. The fault current in the rotor windings and the overvoltage in the DC bus are limited due to the proposed control strategy.

Simulations under Matlab/Simulink environment were performed to compare the voltage dips effect on the wind generation system using the two strategies already developed.

References

[1] Synergrid, Creux de tension : Comment se protéger contre l'inévitable ? la fédération des gestionnaires de réseau électricité et gaz, Belgique. (Book chapter)

[2] S. El Aimani, " Modélisation de différentes technologies d'éoliennes intégrées dans un réseau de moyenne tension ", Sciences et technologies, Lille, 2016. (Thesis)

[3] S. Mokrane, "Modélisation et Commande d'un aérogénérateur à Machine Asynchrone à Double Alimentation en vue de simulation des problèmes de cogénération", diplôme maîtrise en ingénierie. Université du Québec, 2013. (Thesis)

[4] A. Essadki, Modélisation du moteur asynchrone en régime transitoire", Université Mohamed V-Rabat. (Course)

[5] S. El Aimani, "Practical Identification of a DFIG based wind generator model for grid assessment", IEEE International Conference on Multimedia Computing and Systems (ICMCS), pp. 278–285, 2009. (Conference paper)

[6] A. Boukhriss, T. Nasser, A. Essadki, "Linear Active Disturbance Rejection Control applied for DFIG based Wind Energy Conversion System", International Journal of Computer Science Issues (IJCSI), vol. 10, no 2, p. 391-399, 2013. (Article)

[7] A. Boukhriss, A. Essadki, A. Bouallouch, "Maximization of generated power from wind energy conversion systems using a doubly fed induction generator with active disturbance rejection control", Complex Systems (WCCS), Second World Conference on. IEEE, pp. 330-335, 2014. (Conference paper)

[8] R. Chakib, A. Essadki, M. Cherkaoui, "Active Disturbance Rejection Control for Wind System Based on a DFIG", World Academy of Science, Engineering and Technology, International Journal of Electrical, Computer, Energetic, Electronic and Communication Engineering, vol. 8, no 8, pp. 1306-1315, 2014. (Article)

[9] S. El Aimani, B. Francois, F Minne, B Robyns, “Modelling and simulation of doubly fed induction generators for variable speed wind turbines integrated in a distribution network”, 10th European Conference on Power Electronics and Applications (EPE 2003), Toulouse, France (Conference paper)

[10] M. Nadour, A. Essadki, T. Nasser, “Comparative Analysis between PI & Backstepping Control Strategies of DFIG Driven by Wind Turbine”, Internatıonal Journal of Renewable Energy Research (IJRER), vol. 7, no. 3, 2017. (Article)

[11] M.B.C Salles, A.J.S Filho and A.P.Grilo, “A Study on the Rotor Side Control of DFIG-based Wind turbine during Voltage Sags without Crowbar System” International Conference on Renewable Energy Research and Applications, ICRERA, 2013. (Conference paper).

[12] E.Aydin, A. Polat, L.T.E Ergene, “Vector Control Of DFIG n Wind Power Application” International Conference on Renewable Energy Research and Applications, ICRERA, 2016. (Conference paper)

[13] M. Ferrari, “GSC control strategy for harmonic voltage elimination of grid-connected DFIG wind turbine” International Conference on Renewable Energy Research and Applications, ICRERA, 2016. (Conference paper)

[14] A.G. Aissaoui, A. Tahour, M. Abid, N. Essounbouli, F. Nollet, “Using Neuro Fuzzy PI Techniques in Wind Turbine Control” International Conference on Renewable Energy Research and Applications, ICRERA, 2013. (Conference paper).